

## Catalysis Communication 100 (2017) 10-14

### Zr-modified hierarchical mordenite as heterogeneous catalyst for glycerol esterification

Margarita Popova<sup>a,\*</sup>, Hristina Lazarova<sup>a</sup>, Yuri Kalvachev<sup>b</sup>, Totka Todorova<sup>b</sup>, Ágnes Szegedi<sup>c</sup>, Pavletta Shestakova<sup>a</sup>, Gregor Mali<sup>d</sup>, Venkata D.B.C. Dasireddy<sup>d</sup>, Blaž Likozar<sup>d</sup>

<sup>a</sup> Institute of Organic Chemistry with Centre of Phytochemistry, Bulgarian Academy of Sciences, 1113 Sofia, Bulgaria

<sup>b</sup> Institute of Mineralogy and Crystallography, Bulgarian Academy of Sciences, 1113 Sofia, Bulgaria

<sup>c</sup> Research Centre for Natural Sciences, Institute of Materials and Environmental Chemistry, Hungarian Academy of Sciences, 1117 Budapest, Hungary

<sup>d</sup> National Institute of Chemistry, 1001 Ljubljana, Slovenia

\* Corresponding author at: Institute of Organic Chemistry with Centre of Phytochemistry, Acad. G. Bonchev str. Bl. 9, 1113 Sofia, Bulgaria. E-mail address: [mpopova@orgchm.bas.bg](mailto:mpopova@orgchm.bas.bg) (M. Popova).

#### Abstract

Hierarchical mordenite catalysts were prepared by HF and NH<sub>4</sub>F etching. Materials' zirconia modification was performed by incipient wetness impregnation in order to vary surface acidity type and strength. XRD, N<sub>2</sub> physisorption, solid-state NMR and UV–Vis spectroscopies were applied for characterization. Acidic properties of the obtained materials were investigated by TPD of adsorbed ammonia and FT-IR spectra of adsorbed pyridine. Catalytic performance was studied for the glycerol esterification with acetic acid. Zr increased reaction turnover activity compared to raw zeolite substrate due to abundant Brønsted and Lewis moiety presence. The demonstrated biomass valorization processes to bio-based platform chemicals are of interest, as they employ biodiesel production waste.

Keywords: Renewable glycerol esters, Biodiesel production waste, Hierarchical zeolite materials, Bio-based chemicals conversion, Chemical reaction engineering

## 1. Introduction

The increasing demand for energy, chemicals and materials in our society has led research activity towards the development of green technologies, based on renewable resources. Food waste is one of those renewable sources of carbon. Biofuels are an attractive alternative to fossil fuels due to their positive influence on the environment and the fact that they are produced from renewable sources. The production of biodiesel on an industrial scale is achieved through homogeneously catalyzed esterification. The use of refined oil and fats (first generation raw materials) has led to a high cost of the end product and contradiction food/fuels. The production of biofuels on the basis of waste has given research a new spur due to the low cost of the initial raw material, as well as the desire to utilize waste and solve the economic, environmental and social problems. Used cooking oil (UCO) is currently one of the most attractive feedstocks for the production of biodiesel [1–5], mostly due to the low market value of the feedstock. Glycerol is generated as a byproduct in conventional biodiesel production and can be converted to various valuable chemicals through numerous routes such as etherification [6], hydrogenolysis [7], oxidation [8], transesterification [9] and dehydration [10]. Besides, glycerol can be esterified with acetic acid to obtain valuable products of mono-, di- and triacetyl glycerol (named as MAG, DAG and TAG, respectively), which have found versatile industrial applications [11]. MAG and DAG have applications in cosmetics, medicines and as a starting monomer for the production of biodegradable polyesters [1,11]; whereas TAG has application as a biodiesel additive [12]. Traditionally, glycerol esterification with acetic acid is performed over conventional acids as homogeneous catalysts [11]. A major drawback to using homogeneous catalysts is that they lead to serious technical and environmental problems. Therefore, employing heterogeneous acid catalysts can contribute to overcome these drawbacks [1,11,13–16]. Due to their stronger Brønsted acidity than conventional solid acids like mixed oxides and zeolites, Keggin type heteropolyacids (HPAs) can be employed instead of classical homogeneous acids [17–29]. Some drawbacks of bulk HPAs like low thermal stability, high solubility in water and polar media and low surface area ( $1\text{--}10\text{ m}^2\text{g}^{-1}$ ) can be improved by functionalizing them into the framework of high surface area porous supports (silica, activated

carbon, zirconia, polymers and acidic ionexchange resin) [11,18,19]. Hierarchical zeolites are good candidates for catalysts and carriers of catalytic active phase due to their high surface area, adjustable structure, chemical and thermal stability [30–32].

Despite the numerous investigations, the problem with the development of highly acidic heterogeneous catalyst for catalytic utilization of food waste and the development of green technologies to obtain valuable chemicals on their basis still exists.

In the present study hierarchical mordenite was prepared by HF and NH<sub>4</sub>F etching and modified with ZrO<sub>2</sub>. The obtained parent, hierarchical and their Zr-analogs were studied in glycerol esterification with acetic acid. The influence of the textural characteristics of the hierarchical zeolites and the type of the formed acidic sites on the activity to produce glycerol esters is discussed.

## 2. Experimental

### 2.1. Synthesis of parent and hierarchical mordenites

Mordenite was synthesized from a suspension with a molar composition 18SiO<sub>2</sub>:Al<sub>2</sub>O<sub>3</sub>:1.24K<sub>2</sub>O:1.21Na<sub>2</sub>O:22.5H<sub>2</sub>O to which are added 5 wt% mordenite crystals as seed. The crystallization was performed in stainless-steel teflon-lined autoclave under autogenous static conditions for 18 h at 180°C. The obtained highly crystalline mordenite is used for post-synthetic acid treatments with hydrofluoric acid and ammonium fluoride. After that, the samples were converted in H-form by treatment with 1 M solution of ammonium nitrate at 373 K for 24 h and subsequent centrifugation, washing and calcination at 450 °C [33].

### 2.2. Functionalization of the parent and hierarchical mordenite by ZrO<sub>2</sub>

An incipient wetness impregnation technique with ZrCl<sub>2</sub> (99%, Aldrich) was applied for loading of 15 wt% metal oxide. In a typical experiment 1 g of mordenite samples were mixed with 1 ml aqueous solution of ZrCl<sub>2</sub> at room temperature. The precursor salt was decomposed in air at 500 °C for 2 h. Samples were designated as ZrM (M = parent mordenite) and Zr/M1 (M1 = hierarchical mordenite).

### 2.3. Characterization

The X-ray diffraction (XRD) powder patterns were recorded on diffractometer d2 phaser (Bruker) with CuK $\alpha$  radiation, working at acceleration 30 kV and current 10 mA.

The scanning electron microscopy (SEM) analyses were carried out on a Philips 515 instrument working at 20 kV accelerating voltage.

Nitrogen adsorption-desorption isotherms were obtained with micromeritics ASAP 2010 gas analyzer. Micro- and mesopores contributions were determined by the t-plot method. The surface area was calculated by the BET equation and the mesopore distribution was evaluated by the BJH method.

Temperature programmed desorption of ammonia (NH<sub>3</sub>-TPD) was carried out using a Micromeritics 2920 Autochem II Chemisorption Analyser. In the NH<sub>3</sub>-TPD experiments, the catalyst was pretreated at 500 °C under the stream of helium for 60 min. After that the temperature was then decreased to 80 °C. A mixture of 9.8% NH<sub>3</sub> in He as passed over the catalyst at a flow rate of 25 ml/min for 60 min. The temperature was then raised gradually to 900 °C by ramping at 10 °C/ min under the flow of helium. The quantity of the NH<sub>3</sub> desorbed was calculated from a detailed deconvolution of NH<sub>3</sub>-TPD profile. All solid-state NMR experiments were carried out on a 600 MHz Varian NMR system equipped with a 3.2 mm Varian HX CPMAS probe. Larmor frequencies for <sup>1</sup>H, <sup>29</sup>Si, and <sup>27</sup>Al nuclei were 599.53 MHz, 119.10 MHz, and 156.22 MHz, respectively. For <sup>27</sup>Al magic-angle spinning (MAS) measurements excitation pulse of 0.8  $\mu$ s was used, number of scans was 4000 and repetition delay between scans was 0.5 s. Sample rotation frequency was 12.5 kHz. For <sup>29</sup>Si MAS measurements excitation pulse was 2.2  $\mu$ s, repetition delay was 30 s, and number of repetitions was 1000. In the <sup>1</sup>H-<sup>29</sup>Si cross-polarization MAS (CPMAS) experiment, <sup>1</sup>H excitation pulse of 2.3  $\mu$ s was used.

FT-IR experiments were performed with a Nicolet spectrometer by the self-supported wafer technique with pyridine (Py) as probe molecule. Self-supported pellets were pressed from the samples, placed into the IR cell, heated up to 350 °C in high vacuum (10<sup>-6</sup> mbar) with a rate of 10 °C/min and dehydrated for 1 h. Following 30 min contact with Py at 100 °C the sample was evacuated at 200 °C for 30 min.

## 2.4. Catalytic experiments

Prior to the catalytic experiments the samples were pretreated *exsitu* for 1 h at 140 °C in air. A batch reactor equipped with magnetic stirrer was used to perform the reaction. The reactor was charged with 2 g glycerol and 0.1 g catalyst, glycerol/acetic acid weight ratio = 1:10. The reactor was heated to the desired reaction temperature (100 °C) for 3 h and reflux is used for condensation of the evaporated compounds. The analysis of the reaction products was performed using HP-GC equipped with FID.

## 3. Results and discussion

### 3.1. Physico-chemical properties

The mordenite sample with average particle size 4 µm was used as a parent material [33]. The treatment of zeolite with mixture of HF and NH<sub>4</sub>F results in the formation of bigger pores in the initial zeolite [34]. XRD patterns of the parent sample and the sample treated for 20 min with 0.1 M solution of HF and NH<sub>4</sub>F (Fig. 1) exhibit very high degree of crystallinity. The treatment does not lead to any distortion of the mordenite structure. The XRD reflections for the formation of crystalline ZrO<sub>2</sub> phase is not registered after modification with ZrCl<sub>2</sub> which is an indication for the formation of finely dispersed ZrO<sub>2</sub> phase (Fig. 1).

The SEM micrographs of untreated and treated samples are shown in Fig. 2. It can be seen that the formation of bigger pores in the treated sample occurs. TEM images are also indicative of such changes (Supplementary data, SD1). These observations were described in our previous paper [33].

The textural parameters of the studied samples were determined by the nitrogen physisorption and the data of the parent sample compared with those treated with a 0.1 M solution of hydrofluoric acid are listed in Table 1. The isotherms are type I, which is typical for microporous materials. In contrast to the parent sample in isotherms of treated with solution HF-NH<sub>4</sub>F is registered a greater uptake of nitrogen at high partial pressure due to the additional formed pores. The formed additional pores in this case are two times higher than those in the parent mordenite (1.6 nm for M1 comparing to 0.9 nm for M). Impregnation of the initial and hierarchical mordenite with zirconia (15 wt.%) resulted in a small decrease of surface area and pore volume. Decrease of the pores of hierarchical Zr/M1 is registered but the pore blocking

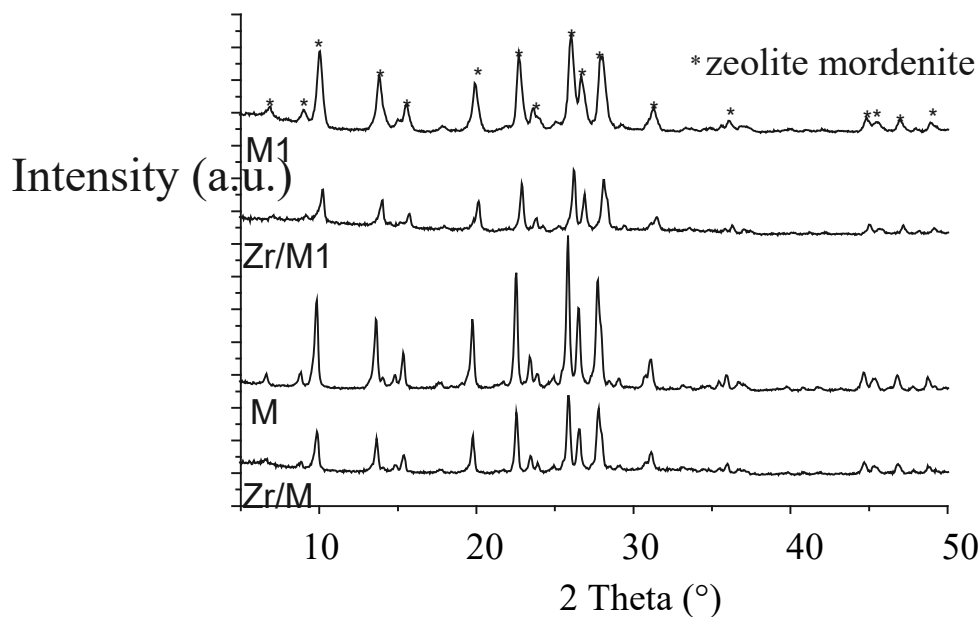


**Fig. 1** XRD patterns of the studied samples

was avoided by the formation of smaller  $ZrO_2$  nanoparticles. Zirconia nanoparticles are immobilized in the hierarchical zeolite matrix due to the interaction with the Brönsted acid sites on the surface. In the case of Zr/ M the pores are not changed after modification with  $ZrO_2$  nanoparticles most probably because they are deposited on the external surface of the parent mordenite.

The registered peaks at the UV–Vis spectra around 200 nm and in the interval 450–500 nm of the parent mordenite have not changed after the acid treatment of zeolite (SD2). The higher intensity of the peak at around 200 nm in the spectra of Zr-modified mordenite is due to the presence of monodispersed Zr atoms surrounded by four oxygen atoms bounded with silicon in mordenite matrix. The additional peak registered at 275 nm is attributed to the presence of nanosized  $ZrO_2$  particles [35], which is more intensive for Zr-modified hierarchical mordenite.  $^{27}Al$  and  $^{29}Si$  NMR spectra were used for characterization of the changes of Si/Al ratio after the etching and impregnation procedures. The  $^{27}Al$  MAS spectra of all samples (SD3) show two signals. The signal at 55 ppm is characteristic for Al atoms in tetra-coordinated framework positions, while the signal at around 0 ppm is typical for the octahedral extra-framework Al

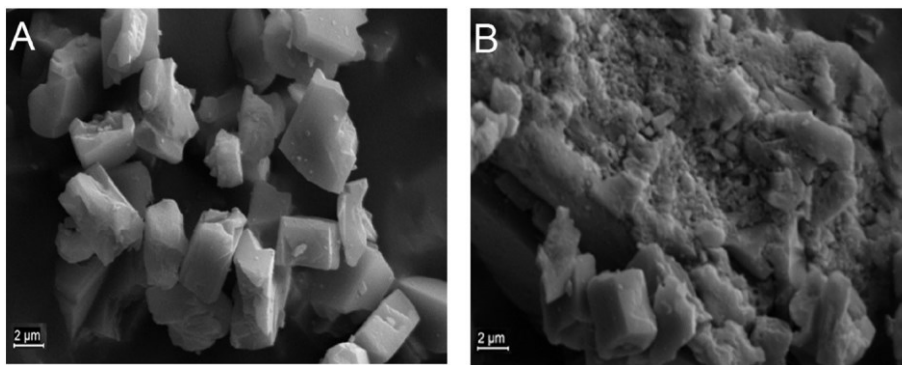


**Fig. 2.** SEM images of parent mordenite (A) and the obtained by acid treatment hierarchical mordenite (B).

sites. The results indicate that the acidic treatment with HF and  $\text{NH}_4\text{F}$ , as well as the modification with zirconia do not result in significant changes in the ratio of framework to extra-framework Al, since the ratio of the integral intensities of the respective signals in the  $^{27}\text{Al}$  spectra is practically the same before and after the treatment.

Fig. 3 shows the  $^{29}\text{Si}$  MAS NMR spectra of the studied samples, where two partially overlapping signals are observed with chemical shifts of  $-102$  and  $-109$  ppm. The first signal can be assigned to Si(1Al) centers ( $\text{Q}^4$ ) and/or Si(1OH) centers ( $\text{Q}^3$ ), whereas the second signal belongs to Si(0Al) centers ( $\text{Q}^4$ ). For all samples the quantity of  $\text{Q}^4$  structures is higher as compared to  $\text{Q}^3$ . The analysis of the deconvoluted spectra shows that the  $\text{Q}^3/\text{Q}^4$  ratio remains the same before and after the modification of the samples M and M1 with Zr. The quantitative analysis of the  $^{29}\text{Si}$  spectra evidenced that for M and Zr/M samples this ratio is lower as compared to M1 and Zr/M1 samples, respectively. More detailed information about the structural environment of the Si centers was obtained from the  $^1\text{H}$ - $^{29}\text{Si}$  CPMAS spectra (cross-polarization magic angle spinning, CPMAS). This technique enables transfer of magnetization from highly sensitive  $^1\text{H}$  to less sensitive  $^{29}\text{Si}$  nuclei resulting in selective enhancement of  $^{29}\text{Si}$  signals of nuclei with neighboring protons e.g.  $\text{Q}^3$  and  $\text{Q}^2$  structures. The broad low intensity signal in the interval from  $-90$  to  $-100$  ppm observed in the CPMAS spectra of the studied samples revealed the presence of small amount of  $\text{Q}^2$  structures [ $\text{Si}(2\text{OH})$ ] in addition to the already detected strong signal for the  $\text{Q}^3$  sites.

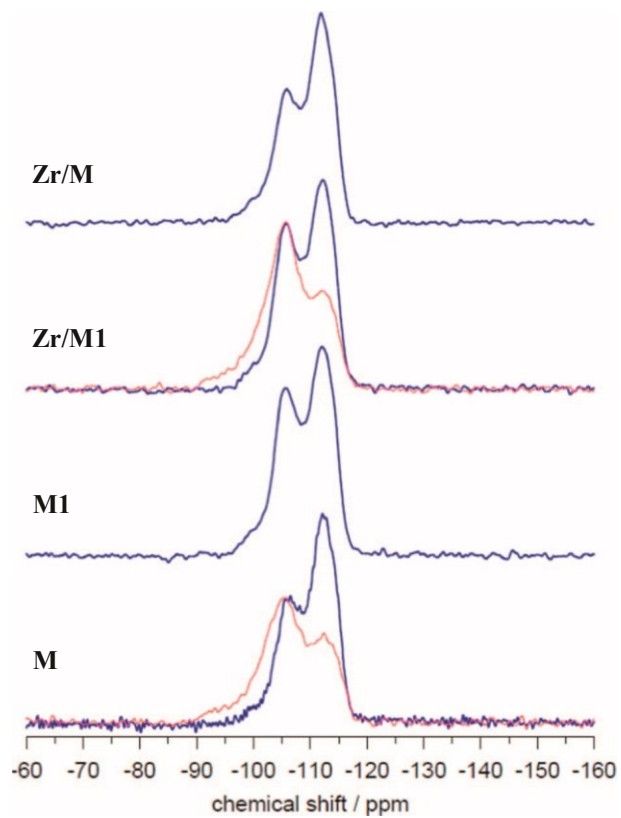


**Fig. 3.**  $^{29}\text{Si}$  MAS (blue line) and  $^1\text{H}$ - $^{29}\text{Si}$  CPMAS (red line) NMR spectra of the studied samples. (For interpretation of the references to colour in this figure legend, the reader is referred to the web version of this article.)



### 3.2. Characterization of the acidic properties

**Table 1**

Textural and acidity properties of the parent mordenite, hierarchical mordenite and their Zr-modified analogs.

| Samples   | M    | M1   | Zr/M | Zr/M1 |
|---|------|------|------|-------|
| BET, m <sup>2</sup> /g                              | 372  | 372  | 302  | 289   |
| Pore volume, cm <sup>3</sup> /g                     | 0.16 | 0.30 | 0.16 | 0.18  |
| Pore size, nm                                       | 0.9  | 1.6  | 0.9  | 1.2   |
| Total amount of NH <sub>3</sub> adsorbed, mmol/g    | 18.6 | 19.5 | 17.0 | 21.8  |
| Up to 175 °C, mmol/g                                | 6.2  | 7.4  | 6.4  | 7.3   |
| 175–510 °C, mmol/g                                  | 8.9  | 8.4  | 7.2  | 10.5  |
| 510–740 °C, mmol/g                                  | 3.5  | 3.7  | 3.4  | 4.0   |
| Brönsted/Lewis ratio, calculated from FT-IR spectra | 1.7  | 1.9  | 0.5  | 0.7   |

*- By TPD of adsorbed ammonia*

TPD of ammonia (Table 1) reveal the presence of the weak, strong and moderate acidic sites on the surface of catalysts which were evidenced by the three desorption peaks: 150–300 °C for weak, 300–600 °C for moderate, and above 600 °C for strong acidic sites, respectively. The experiments show that the modification with Zr of hierarchical mordenite slightly increases the amount of strong acid sites from which the ammonia desorption is registered at 175–510 °C (Table 1). These results together with NMR data are indicative for the additional formation of strong Lewis acid sites.

*- By FT-IR spectra of adsorbed pyridine*

Initial and Zr-modified mordenites show acidic properties, i.e. Lewis and Brönsted acid surface sites can be distinguished (Fig. 4). The

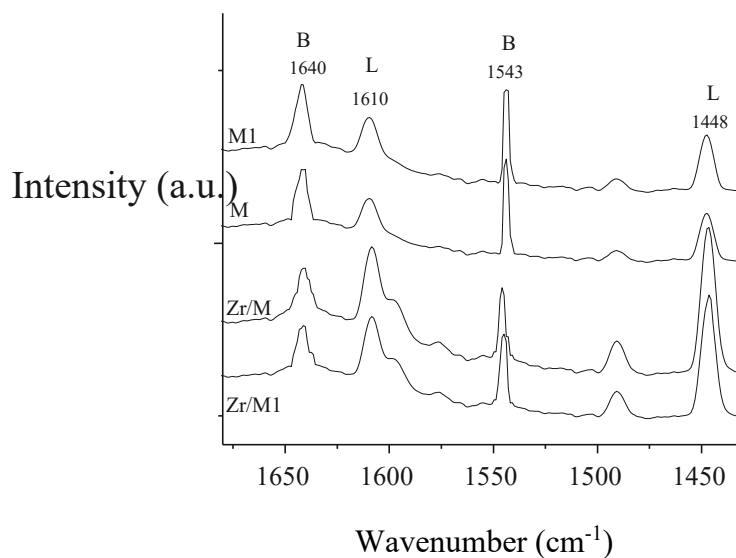


**Fig. 4.** FT-IR spectra of the adsorbed pyridine on the studied samples.

relative amount and nature of these types of acidic species can be determined by FT-IR spectroscopic investigation of adsorbed pyridine (Py). The bands at about 1610 cm<sup>-1</sup>, and 1448 cm<sup>-1</sup> are assigned to Py coordinated to Lewis acid sites (Py-L) (Fig. 4). The protonated Py coordinated to the conjugated base of the solid Brønsted acid (Py-B) gives bands at 1540 cm<sup>-1</sup> and 1640 cm<sup>-1</sup>. The coordinatively unsaturated Zr ions on the surface of zirconia can act as Lewis acid sites. Upon the Zr-modification the intensity of bands characteristic for Lewis acid sites increased, and a small decrease in the Brønsted acid sites of mordenites is registered. The Brønsted/Lewis acid sites ratio for the studied samples is presented in Table 1. The calculated value for Zr/M1 sample (0.7) is an indication for presence of similar amounts of Brønsted and Lewis acid sites.

**Table 2**

Catalytic properties of the parent mordenite, hierarchical mordenite and their Zr-modified analogs at 100 °C and 3 hour reaction time.

| Samples                  | Glycerol conversion, % | Selectivity to MAG, % | Selectivity to DAG, % | Selectivity to TAG, % |
|--------------------------|------------------------|-----------------------|-----------------------|-----------------------|
| M                        | 68.2                   | 33.1                  | 14.6                  | 52.3                  |
| M1                       | 89.3                   | 19.3                  | 17.0                  | 63.7                  |
| Zr/M                     | 74.4                   | 32.2                  | 24.6                  | 43.2                  |
| Zr/M1                    | 93.5                   | 18.4                  | 12.4                  | 69.2                  |
| Spent Zr/M <sup>a</sup>  | 65.1                   | 45.5                  | 30.9                  | 23.6                  |
| Spent Zr/M1 <sup>a</sup> | 90.6                   | 21.5                  | 12.4                  | 66.1                  |

<sup>a</sup> Activity and selectivity in 3 reaction cycles.

### 3.3. Catalytic activity for glycerol esterification with acetic acid on parent, hierarchical mordenite and Zr-modified analogs

Catalytic performance of the parent and hierarchical mordenites and their Zr-modified analogs in esterification of glycerol with acetic acid is presented in Table 2. Acid treatment of the initial mordenite leads to higher catalytic activity in esterification of glycerol most probably because of the larger pores of hierarchical zeolite (1.6 nm for M1 comparing to 0.9 nm for M) and the same acidity after acid treatment (Table 1). Additional modification with zirconia oxide phase results in higher catalytic activity for both catalysts. The presence of strong Brönsted and Lewis acid sites could be the reason for better catalytic performance. Higher catalytic activity to more valuable triacetyl glycerol is registered for M1 and Zr/M1 (Table 2) which are favored in the larger pores of hierarchical mordenite and the presence of strong Brönsted and Lewis acid sites. The high catalytic stability of the Zr/M1 is registered in 3 reaction cycles (Table 2) and it could be assigned to the simultaneous presence of Brönsted and Lewis acid sites and the free access of the reactant's molecules to them in the pores of hierarchical mordenite.

## 4. Conclusion

Hierarchical mordenite was prepared by etching with HF and NH<sub>4</sub>F. Zr-modifications of initial and hierarchical mordenites were prepared by incipient wetness impregnation. The obtained catalysts show high catalytic activity in glycerol esterification with acetic acid and selectivity to valuable triacetyl glycerol. Investigation of the acidic properties of the Zr-modified catalysts revealed that the presence of sufficient amounts of Brønsted and Lewis acid sites with strong acidity is of crucial importance for their catalytic performance. Zr-modified hierarchical mordenite shows the best catalytic performance in the studied reaction, most probably due to the optimal Brønsted/Lewis acid sites ratio and better access to them. The Zr-modified hierarchical mordenite is a highly active, cost effective, stable and reusable catalyst.

## Acknowledgements

Financial support from the COST action TD 1203 and by the NSF of Bulgaria (Contract ДКОСТ 01/5). The authors Yu. Kalvachev and T. Todorova acknowledge the financial support from “Program for career development of young scientists, Bulgarian Academy of Sciences’2016” (Contract No. DFNP 182). The authors Venkata D. B. C. Dasireddy, Blaž Likozar acknowledge the financial support from the Slovenian Research Agency (research core funding No. P2-0152).

## Appendix A. Supplementary data

Supplementary data to this article can be found online at <http://dx.doi.org/10.1016/j.catcom.2017.06.009>.

## References

- [1] Handbook of biofuels production: processes and technologies, University of Córdoba, Spain. University of York, UK, in: R. Luque, J. Campelo, J. Clark (Eds.), Woodhead Publishing Series in Energy No. 15, 2013.
- [2] C.S.K. Lin, L.A. Pfaltzgraff, L. Herrero-Davila, E.B. Mubofu, S. Abderrahim, J.H. Clark, A. Koutinas, N. Kopsahelis, K. Stamatelatos, F. Dickson, S. Thankappan, Z. Mohamed, R. Brocklesby, R. Luque, Energy Environ. Sci. 6 (2013) 426–464.

- [3] J.H. Clark, V. Budarin, Th. Dugmore, R. Luque, Catalytic performance of carbonaceous materials in the esterification of succinic acid, *Catal. Commun.* 9 (2008) 1709–1714.
- [4] D.J. Macquarrie, V. Strelko, M.S. Khayoon, B.H. Hameed, Synthesis of hybrid SBA15 functionalized with molybdophosphoric acid as efficient catalyst for glycerol esterification to fuel additives, *Appl. Catal. A* 433–434 (2012) 152–161.
- [5] F.G. Cirujano, A. Corma, F.X. Llabrés i Xamena, Conversion of levulinic acid into chemicals: Synthesis of biomass derived levulinate esters over Zr-containing MOFs, *Chem. Eng. Sci.* 124 (2015) 52–60.
- [6] K. Wilson, A.F. Lee, D.J. Macquarrie, J.H. Clark, Structure and reactivity of sol–gel sulphonic acid silicas, *Appl. Catal. A* 228 (2002) 127–133.
- [7] R. van Grieken, J.A. Melero, G. Morales, Fries rearrangement of phenyl acetate over sulfonic modified mesostructured SBA-15 materials, *Appl. Catal. A* 289 (2005) 143–152.
- [8] D. Liang, J. Gao, H. Sun, P. Chen, Z. Hou, X. Zheng, Novel fine-disperse bimetallic Pt-Pd/Al<sub>2</sub>O<sub>3</sub> catalysts for glycerol oxidation with molecular oxygen, *Appl. Catal. B* 106 (2011) 423–432.
- [9] S. Shylesh, S. Sharma, S.P. Mirajkar, A.P. Singh, Silica functionalised sulphonic acid groups: synthesis, characterization and catalytic activity in acetalization and acetylation reactions, *J. Mol. Catal.* 212 (2004) 219–228.
- [10] M. Trejda, K. Stawicka, M. Ziolk, New catalysts for biodiesel additives production, *Appl. Catal. B* 103 (2011) 404–412.
- [11] Ch.-H. (Clayton) Zhou, J.N. Beltramini, Y.-X. Fana, G.Q. (Max) Lu, Chemoselective catalytic conversion of glycerol as a biorenewable source to valuable commodity chemicals, *Chem. Soc. Rev.* 37 (2008) 527–549.
- [12] M.L. Testa, V. La Parola, L.F. Liotta, A.M. Venezia, Screening of different solid acid catalysts for glycerol acetylation, *J. Mol. Catal.* 367 (2013) 69–76.
- [13] J.A. Sánchez, D.L. Hernández, J.A. Moreno, F. Mondragón, J.J. Fernández, Alternative carbon based acid catalyst for selective esterification of glycerol to acetylglycerols, *Appl. Catal. A* 405 (2011) 55–60.
- [14] K. Jagadeeswaraiyah, M. Balaraju, P.S. Sai Prasad, N. Lingaia, Selective esterification of glycerol to bioadditives over heteropoly tungstate supported on Cs-containing zirconia catalysts, *Appl. Catal. A* 386 (2010) 166–170.

- [15] M.S. Khayoon, B.H. Hameed, Acetylation of glycerol to biofuel additives over sulfated activated carbon catalyst, *Bioresour. Technol.* 102 (2011) 9229–9235. [16]
- [16] T. Borrego, M. Andrade, M.L. Pinto, A. Rosa Silva, A.P. Carvalho, J. Rocha, Cristina Freire, J. Pires, Physicochemical characterization of silylated functionalized materials, *J. Colloid Interface Sci.* 344 (2010) 603–610.
- [17] D. Pérez-Quintanilla, A. Sánchez, I. del Hierro, M. Fajardo, I. Sierra, Preparation, characterization, and  $Zn^{2+}$  adsorption behavior of chemically modified MCM-41 with 5-mercapto-1-methyltetrazole, *J. Colloid Interface Sci.* 313 (2007) 551–562.
- [18] E. Li, Z.P. Xu, V. Rudolph, MgCoAl-LDH derived heterogeneous catalysts for the ethanol transesterification of canola oil to biodiesel, *Appl. Catal. B* 88 (2009) 42–49.
- [19] M.S. Khayoon, M.A. Olutoye, B.H. Hameed, Utilization of crude karanj (*Pongamia pinnata*) oil as a potential feedstock for the synthesis of fatty acid methyl esters, *Bioresour. Technol.* 111 (2012) 175–179.
- [20] A. Corma, G.W. Huber, L. Sauvanaud, P. O'Connor, Biomass to chemicals: catalytic conversion of glycerol/water mixtures into acrolein, reaction network, *J. Catal.* 257 (2008) 163–171.
- [21] H. Liu, L. Su, F. Liu, C. Li, U.U. Solomon, Cinder supported  $K_2CO_3$  as catalyst for biodiesel production, *Appl. Catal. B* 106 (2011) 550–558.
- [22] K. Pathak, K.M. Reddy, N.N. Bakhshi, A.K. Dalai, Catalytic conversion of glycerol to value added liquid products, *Appl. Catal. A* 372 (2010) 224–238.
- [23] F.A.F. Frusteri, G. Bonura, C. Cannilla, L. Spadaro, O. Di Blasi, Catalytic etherification of glycerol by tert-butyl alcohol to produce oxygenated additives for diesel fuel, *Appl. Catal. A* 367 (2009) 77–83.
- [24] A. Bienholz, H. Hofmann, P. Claus, Selective hydrogenolysis of glycerol over copper catalysts both in liquid and vapour phase: correlation between the copper surface area and the catalyst's activity, *Appl. Catal. A* 391 (2011) 153–157.
- [25] D. Liang, J. Gao, H. Sun, P. Chen, Z. Hou, X. Zheng, Selective oxidation of glycerol with oxygen in a base-free aqueous solution over MWNTs supported Pt catalysts, *Appl. Catal. B* 106 (2011) 423–432.
- [26] J. Li, T. Wang, *Chem. Eng. Process. Process Intensif.* 49 (2010) 530–535.

- [27] E. Yoda, A. Ootawa, Dehydration of glycerol on H-MFI zeolite investigated by FT-IR, *Appl. Catal. A* 360 (2009) 66–70.
- [28] P. Ferreira, I.M. Fonseca, A.M. Ramos, J. Vital, J.E. Castanheiro, Glycerol acetylation over dodecatungstophosphoric acid immobilized into a silica matrix as catalyst, *Appl. Catal. B* 91 (2009) 416–422.
- [29] P.C. Smith, Y. Ngothai, Q. Dzuy Nguyen, B.K. O'Neill, Improving the low-temperature properties of biodiesel: methods and consequences, *Renew. Energy* 35 (2010) 1145–1151.
- [30] J. Kowalska-Kus, A. Held, M. Frankowski, K. Nowinska, Solketal formation from glycerol and acetone over hierarchical zeolites of different structure as catalysts, *J. Mol. Catal. A* 426 (2017) 205–212.
- [31] D.P. Gamliel, H. Je Cho, W. Fan, J.A. Valla, On the effectiveness of tailored mesoporous MFI zeolites for biomass catalytic fast pyrolysis, *Appl. Catal. A* 522 (2016) 109–119.
- [32] K. Zhang, M.L. Ostraat, Innovations in hierarchical zeolite synthesis, *Catal. Today* 264 (2016) 3–15.
- [33] Y. Kalvachev, T. Todorova, D. Nihtianova, H. Lazarova, M. Popova, Fluoride etching of mordenite and its influence on catalytic activity, *J. Mater. Sci.* 52 (2017) 5297–5308.
- [34] Zh. Qin, J.-P. Gilson, V. Valtchev, Mesoporous zeolites by fluoride etching, *Chem. Eng.* 8 (2015) 1–6.
- [35] J. Joo, T. Yu, Y.W. Kim, H.M. Park, F. Wu, J.Z. Zhang, T. Hyeon, Multigram scale synthesis and characterization of monodisperse tetragonal zirconia nanocrystals, *J. Am. Chem. Soc.* 125 (2003) 6553–6557.